Metabolic and functional evaluation of diabetic cardiomyopathy using MR Spectroscopy and MR Imaging

Bizino, M.B.

Citation

Bizino, M. B. (2022, November 16). *Metabolic and functional evaluation of diabetic cardiomyopathy using MR Spectroscopy and MR Imaging*. Retrieved from https://hdl.handle.net/1887/3486006

Version:	Publisher's Version
License:	Licence agreement concerning inclusion of doctoral thesis in the Institutional Repository of the University of Leiden
Downloaded from:	https://hdl.handle.net/1887/3486006

Note: To cite this publication please use the final published version (if applicable).

Chapter 4

High Spatial Resolution Coronary Magnetic Resonance Angiography at 7 T: Comparison with Low Spatial Resolution Bright Blood Imaging

Bizino MB, Bonetti C, van der Geest RJ, Versluis MJ, Webb AG, Lamb HJ

Invest Radiol. 2014 May;49(5):326-30.

Abstract

Objectives

The aim of this study was to compare bright blood high spatial resolution (HR) coronary magnetic resonance angiography (MRA) with low spatial resolution (LR) bright blood coronary MRA at 7 T.

Materials and methods

Twenty-four healthy volunteers underwent navigator-gated
3-dimensional imaging of the right coronary artery at 7 T using 2 sequences: HR bright blood and LR bright blood. Image postprocessing involved newly developed multiplanar reformatting to straighten the right coronary artery. Image quality was determined by vessel edge sharpness, signal-to-noise ratio, contrast-to-noise ratio, visible vessel length, and vessel diameter.

Results

Vessel edge sharpness was statistically significantly higher in HR as compared with LR (0.57 ± 0.1 vs 0.46 ± 0.06; P < 0.001), at the cost of lower signal-to-noise ratio (HR, 32.9 ± 11.0 vs LR, 112.5 ± 48.9; P < 0.001) and contrast-to-noise ratio (HR, 17.9 T 7.4 vs LR, 50.5 ± 26.1; P < 0.001). Visible vessel length and vessel diameter were similar for both sequences (P > 0.05).

Conclusions

High spatial resolution bright blood coronary MRA at 7 T is feasible and improves vessel edge sharpness as compared with LR bright blood imaging.

Introduction

The most commonly used diagnostic tools for detection of significant coronary artery disease are x-ray-based techniques such as invasive coronary angiography (CAG) and noninvasive computed tomography angiography (CTA).[1] Both CAG and CTA require administration of iodinated contrast and exposure of the patient to ionizing radiation.

Magnetic resonance angiography (MRA) is a noninvasive radiation-free imaging technique and does not require contrast administration. Magnetic resonance angiography has been shown to allow reliable detection of significant proximal coronary artery stenosis[2,3] with equal diagnostic accuracy as compared with CTA.[4] The small size of coronary arteries, tortuosity, complex anatomy, as well as cardiac and respiratory motion make coronary MRA technically challenging and relatively time-consuming.

In terms of the effect of field strength on image quality and diagnostic value, Sommer et al[5] demonstrated an increase in signal-to-noise ratio (SNR) and contrast-to-noise ratio (CNR) of coronary MRA at 3 T as compared with 1.5 T. High SNR and CNR ensure good vessel conspicuity but do not necessarily result in higher diagnostic accuracy.[5] Besides vessel conspicuity, well-defined borders, specified as vessel edge sharpness (VES), are necessary for precise detection of significant coronary artery stenosis. By using the increase in SNR at higher magnetic resonance field strength for higher spatial resolution, it might be possible to increase VES.

Therefore, ultrahigh field MRA seems an interesting option to further increase SNR and spatial resolution. Despite practical and physics-related technical challenges,[6] several groups have achieved whole-heart imaging at 7 T.[7-10] Previously, van Elderen et al[11,12] reported on increased SNR, CNR, and VES of the right coronary artery (RCA) at 7 T as compared with 3 T. Diagnostic accuracy might be further increased by implementing higher spatial resolution imaging protocols that increase VES. Therefore, the purpose of the present study was to compare high spatial resolution (HR) bright blood coronary MRA at 7 T with a low spatial resolution (LR) bright blood sequence.

Materials and methods

The study was approved by the hospital institutional review board and all volunteers provided written informed consent before the study. Twenty-four healthy volunteers (16 women, 8 men; mean ± SD age, 26.9 ± 11.0 years; mean ± SD body mass index [BMI], 22.4 ± 2.6 kg/m^2) underwent navigator-gated 3-dimensional (3D) MRA of the RCA on a whole-body 7 T system (Achieva, Philips Healthcare, Best, the Netherlands).

Image acquisition

A custom-built quadrature 2-element surface transmit/receive coil was used. The coil consisted of loops, each 18 cm in diameter, segmented by 8 series capacitors and overlapped to minimize mutual inductance. This coil was slightly larger as compared with previously published studies[10-12] to improve volumetric coverage.

First, non-electrocardiogram-triggered scout images were acquired in coronal, transverse, and sagittal orientations to plan subsequent images. Second, electrocardiogram-triggered, breath-hold multisection transverse cine scout imaging was performed for both determination of the period of minimal coronary motion (mean ± SD trigger delay, 335.68 ± 33.87 milliseconds) and volume targeting of the 3D stack parallel to the mid-diastolic RCA. Finally, volume-targeted coronary MRAs were acquired with 2 different imaging protocols. Table 1 summarizes imaging parameters for both coronary MRA sequences. The in-plane field of view for both sequences was 420 x 270 mm. The HR sequence had a coverage of 21 mm; voxel size of 0.45 x 0.45 x 1.2 mm, which was further reduced to 0.31 x 0.31 x 0.6 mm by interpolation to approach spatial resolution of invasive CAG; matrix size of 932 x 604; and 35 slices were acquired with an echo time of 1.64 ± 0.16 milliseconds and repetition time of 4.76 ± 0.16 milliseconds. The LR sequence had a coverage of 30 mm; voxel size of 0.82 x 0.82 x 2 mm, which was interpolated to 0.82 x 0.82 x 1.00 mm as previously performed by our group[11]; matrix size of 512 x 312; and 30 slices were acquired with an echo time of 1.3 ± 0.03 milliseconds and repetition time of 4.03 ± 0.04 milliseconds. For both sequences, a flip angle of 15 degrees was used. The total image acquisition shot duration per heartbeat was limited to 115 milliseconds for all sequences to limit the effect of cardiac motion. A pencil beam navigator was positioned on the lung-liver interface to monitor and correct for respiration. A gating window for acceptance of 5 mm was used. Fat suppression was achieved using a spectrally selective adiabatic inversion recovery pulse (inversion time, 200 milliseconds). For both imaging sequences, a first-order local volume shimming at the anatomic level of the RCA was performed. Total scan duration depended on navigator efficiency. Assuming 100% efficiency, the HR sequence took 9 minutes and the LR sequence took 4 minutes to complete.

Table 1. 7 Tesla coronary magnetic resonance angiography acquisition parameters

	High spatial resolution	Low spatial resolution
Number of slices	35	30
Field of view (mm x mm)	420 x 272	420 x 269
Matrix	932 x 604	512 x 312
TR (msec)	4.76 ± 0.16	4.03 ± 0.04
TE (msec)	1.64 ± 0.04	1.3 ± 0.03
TD (msec)	335.68 ± 33.87	335.68 ± 33.87
Flip angle (degree)	15	15
NSA	1	1
Acquired voxel (mm)	0.45 x 0.45 x 1.2	0.82 x 0.86 x 2.00
Reconstructed voxel (mm)	0.31 x 0.31 x 0.6	0.82 x 0.82 x 1.00

All images were acquired using a 3D gradient echo sequence and a custom-built quadrature coil (see methods section for details). TR = repetition time, TE = echo time, TD = trigger delay, NSA = number of signal averages, FOV = field of view, SPAIR = spectrally selective adiabatic inversion recovery.

Image post-processing

Images were processed using MASS research software version 2012-EXP (Leiden University Medical Center, Leiden, The Netherlands) including newly developed coronary image analysis. Image post-processing and analysis were performed by C.B.

Coronary MRA requires a stack of thin-slab 3D volume-targeted acquisitions. The slabs embrace contiguous sections to enable visualization of the entire tortuous coronary artery. A new approach for analysis of image quality parameters such as VES, SNR, and CNR involving multiplanar reformatting (MPR) was developed. Figure 1 shows the image post-processing in detail. Identification of the RCA was performed manually by placing points of interest in the coronary segment with maximum signal intensity of the blood (Fig. 1A). Vessel length was then automatically calculated by the software. Figure 1B shows a cross-section perpendicular to the coronary (transverse MPR). These cross-sections were then aligned. To produce a straightened RCA, radial MPR was performed (Fig. 1C). It was empirically determined that 18 was the minimum number of reformatting planes needed for optimal preservation of coronary anatomic information. The radial MPR with highest contrast along the vessel was chosen (Fig. 1D). This final image was used for manual placement of regions of interest (ROIs) such as blood and epicardial fat (Fig. 1E). The ROI automatically subdivided into sub-ROIs, which were tuned to fit the 3 anatomic regions: blood vessel and left and right epicardial fat. The ROI was displayed as an elongated rectangle or pixel matrix n times m (with n G m) enabling the identification of a maximum of m chords all with length equal to n. Chords were resampled by linear interpolation using a fixed number of 20 pixels, resulting a mean pixel size of 0.3 mm (ROI width was, on average, 6 mm). Using this approach in both sequences, images were quantitatively analyzed with a similar reconstructed pixel size. One hundred chords were set along the length of the RCA, which were subsequently divided into 20 groups of 5 chords. The software then calculated, for each group of 5 chords, an average crossed intensity profile (CIP). Twenty CIPs were set out in a graph to designate the vessel border (Fig. 1F). The average CIP was used to generate data for the analysis of VES.

Data analysis

The signal of blood (S_{blood}) was calculated as the mean signal of all 20 ROIs. To minimize the effect of structures other than fat in the ROIs of left and right epicardial fat, the average signal of fat (S_{fat}) was weighted by the standard deviations (R) of the right and left components of epicardial fat ROIs (see Equation 1).

(1) $S_{fat} = ((S_{fat\text{-}left} / \sigma_{fat\text{-}left}) + (S_{fat\text{-}right} / \sigma_{fat\text{-}right})) / ((1 / \sigma_{fat\text{-}left}) + (1 / \sigma_{fat\text{-}right}))$

Similarly, the averages of the rising and decaying blood signal intensity along the intensity profiles, that is, the slope (SL), were weighted for the standard deviations of the signal in right and left ROIs (see Equation 2).

(2) $SL = ((SL_{up} / \sigma_{up}) + (SL_{down} / \sigma_{down})) / ((1 / \sigma_{up}) + (1 / \sigma_{down}))$

As described elsewhere,[13] Equation 3 was used to calculate VES. This equation corrects for differences in signal intensity. The average of the maximum signal of blood in each of the 20 sub-ROIs was calculated (S_{blood} max). The averages of 40 sub-ROIs gave rise to S_{fat} min. A VES of 1.0 reflects a full transition of S_{blood} to S_{fat} over a 1.0-mm distance, whereas a VES of 0.0 represents the absence of a transition.

(3) $VES = SL / (S_{blood\ max} – S_{fat\ min})$

Noise (N) was assessed by determination of the standard deviation of the signal intensity in an ROI positioned anterior to the chest wall. Signal-to-noise ratio was calculated by dividing S_{blood} by N and CNR was defined as the difference between S_{blood} and S_{fat} divided by N. Vessel diameter was assessed as full-width at half-maximum of the CIPs.

Statistical analysis

Data are presented as mean ± SD. To evaluate significant differences of image quality parameters between coronary MRA sequences, a Wilcoxon signed-rank test was used. A cutoff value of 0.05 was considered statistically significant. The null hypothesis was that population means are equal among the variables. SPSS statistics version 20.0 (IBM) was used for data management and calculation.

Results

Total time in the scanner for each volunteer was approximately 40 minutes. Scanning times were 877 seconds (14:37 minutes) and 435 seconds (7:15 minutes) for HR and LR, respectively. The average navigator efficiencies were 54% in LR and 60% in HR. Heart rate had a mean value of 65 beats per minute and was not significantly different between sequences (P = 0.988). Figure 2 shows coronary MRA images acquired with both sequences in a single volunteer. Figure 3 shows an example of the HR versus LR coronary MRA in a 61-year-old male volunteer with a BMI of 27.6 kg/m^2 and an 18-year old woman with a BMI of 27.6 kg/m^2 to reflect feasibility in the elderly and obese individual, respectively. Figure 4 depicts in detail the anatomy of the proximal and middle segments of the RCA as assessed by HR imaging.

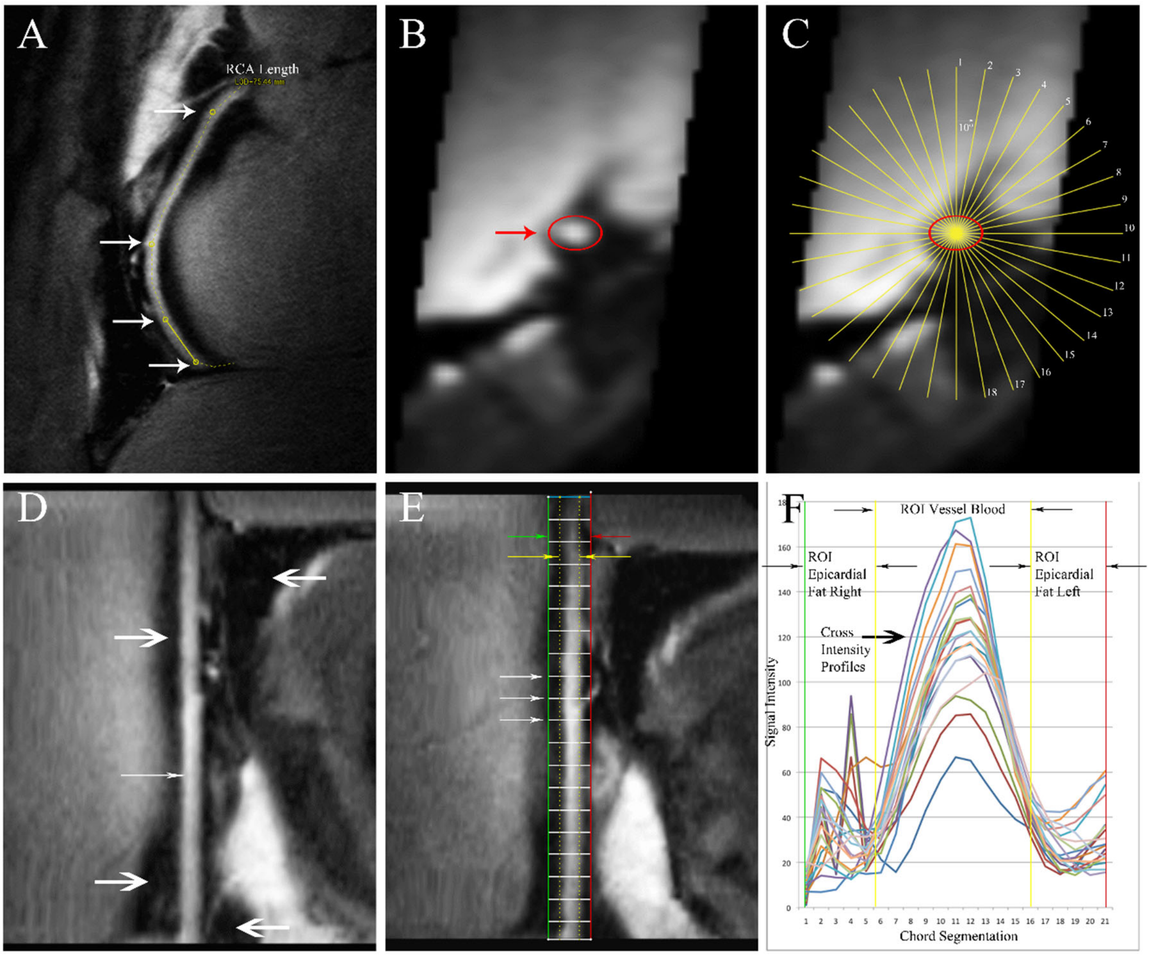

Figure 1. Post-processing steps involved in multi-planar reformatting (MPR), selection of the region of interest (ROI) and crossed intensity profile (CIP). A, The right coronary artery (RCA) is identified (dots depict the points of interest along the coronary segment). This procedure is used to estimate vessel length. B, A cross-section of the RCA (ellipse) produced by transverse-MPR. C, From the center of the RCA a radial-MPR is produced from eighteen reformatting planes with 10- spacing. D, Straightened RCA (thin arrow). The cross-section showing the best blood / fat contrast along the vessel is chosen. The thick arrows indicate the suppressed signal of epicardial fat. E, The ROI's are outlined in the straightened RCA. The region between the two vertical lines is manually placed to incorporate both RCA and epicardial fat. The dotted lines divide the ROI in three sub-ROI's which can be precisely tuned to fit the three anatomic regions: blood vessel and left and right epicardial fat. Twenty-one chords (horizontal lines) are displayed along the length of the RCA. F, This figure shows the CIP plotted against the chord segmentation. The area of the graph is divided manually into three parts corresponding to the sub-ROI's.

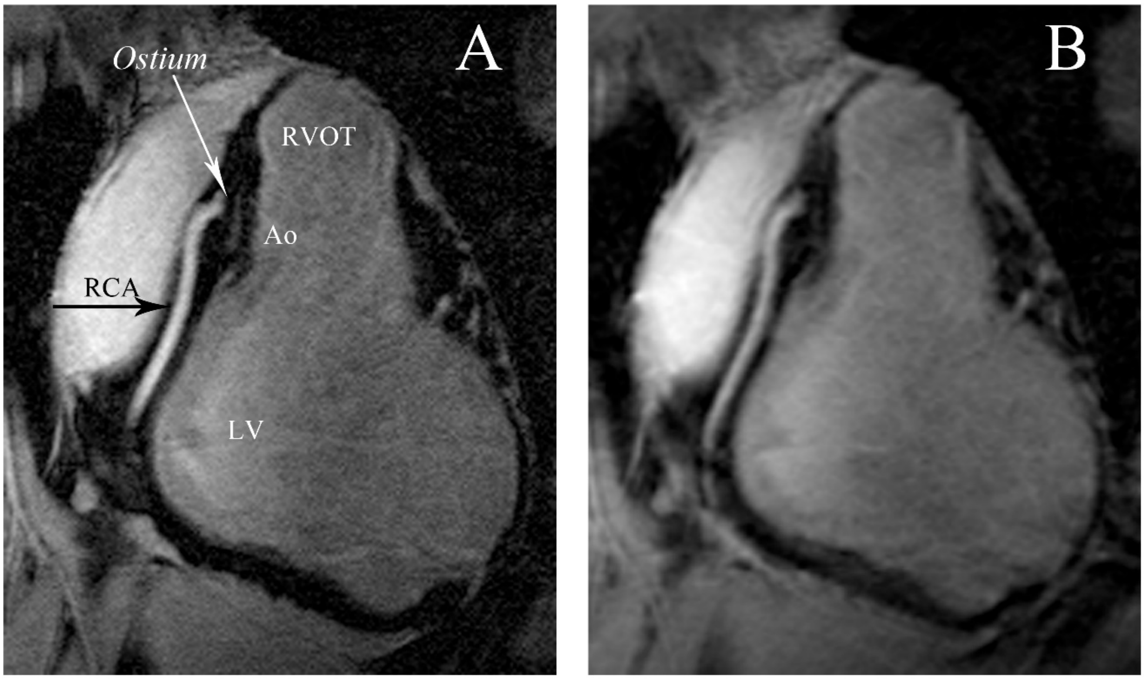

Figure 2. Magnetic resonance angiograms of the RCA in a single healthy volunteer obtained with both sequences. A, HR sequence produces an image with clearly defined vessel borders; the contrast between blood and epicardial fat enables good identification of the RCA. Several structures can be identified in this image: the ostium and a portion of the RCA. B, The LR image shows good fat suppression and vessel conspicuity. RVOT indicates right ventricular outflow tract; Ao, aortic root; LV, left ventricle.

To quantitatively compare image quality of HR and LR sequences, VES, SNR, and CNR were assessed. The HR sequence had significantly higher VES than the LR sequence did (0.57 ± 0.10 vs 0.46 ± 0.06; $P < 0.001$). As expected, HR images had lower SNR (32.9 ± 11.0) as compared with LR images (112.5 ± 48.9; $P < 0.001$). Contrast-to-noise ratio was, on average, 17.9 ± 7.4 in the HR sequence images, which was also significantly lower than the LR sequence, which had a CNR of 50.5 ± 26.1 ($P < 0.001$). Right coronary artery visible vessel length tended to be higher in the HR sequence, although it was not significantly different from that in the LR sequence (83.2 ± 13.0 vs 78.7 ± 12.2 mm; $P = 0.056$). Mean vessel diameter was 3.16 ± 0.8 and 3.3 ± 0.7 mm for HR and LR, respectively, and was not significantly different ($P = 0.179$).

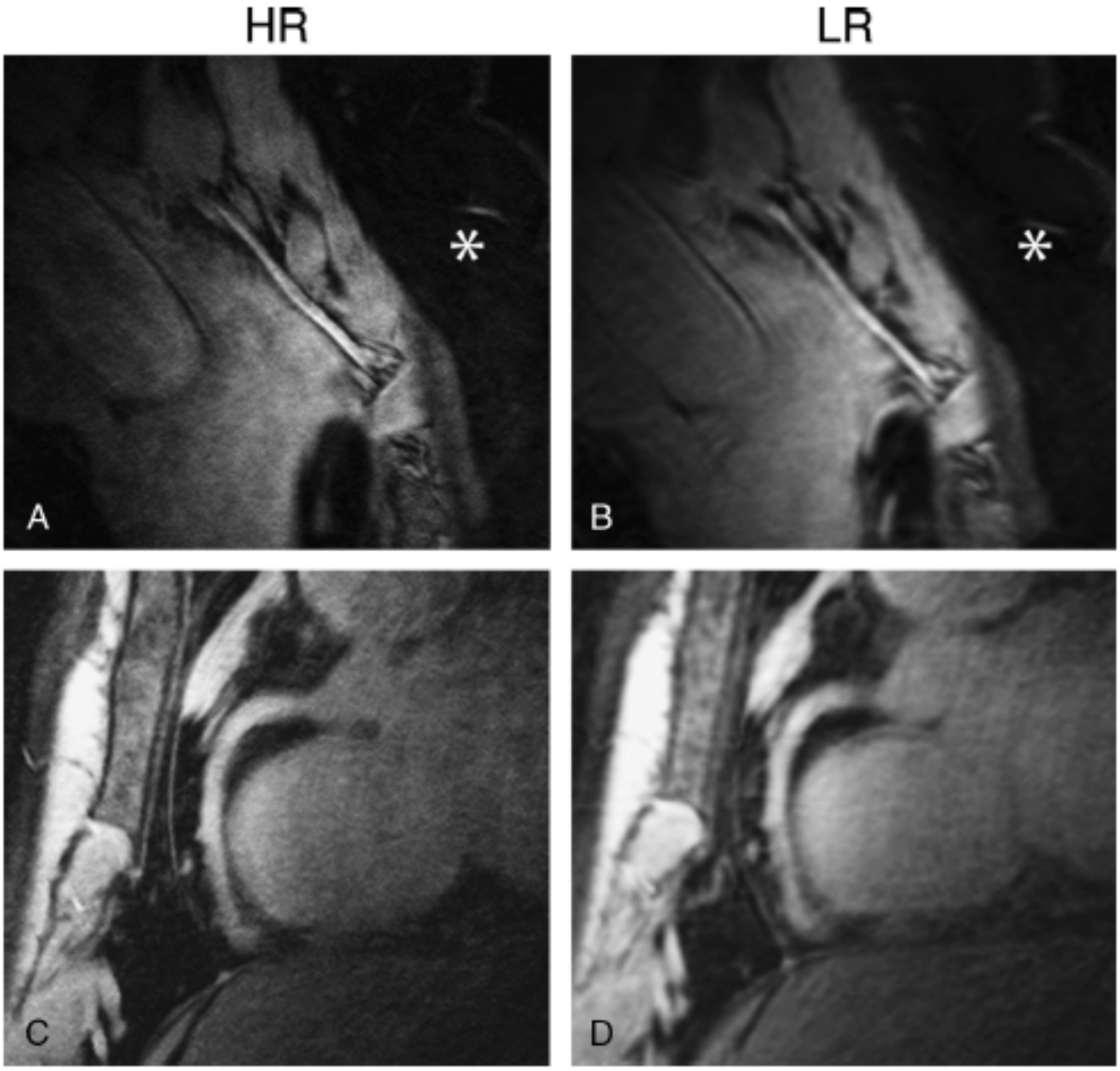

Figure 3. In the upper panel, high (A) and low (B) spatial resolution images of an 18-year-old woman with a BMI of 27.6 kg/m^2 are displayed. The RCA can be visualized well with both sequences. As can be clearly depicted, vessel borders are delineated more sharply in the HR image. Also note abundant subcutaneous adipose tissue (star), indicating that coronary MRA is feasible in obesity. The lower panel (C and D) shows the RCA of a 61-year-old overweight (BMI, 27.6 kg/m^2) but otherwise healthy male subject.

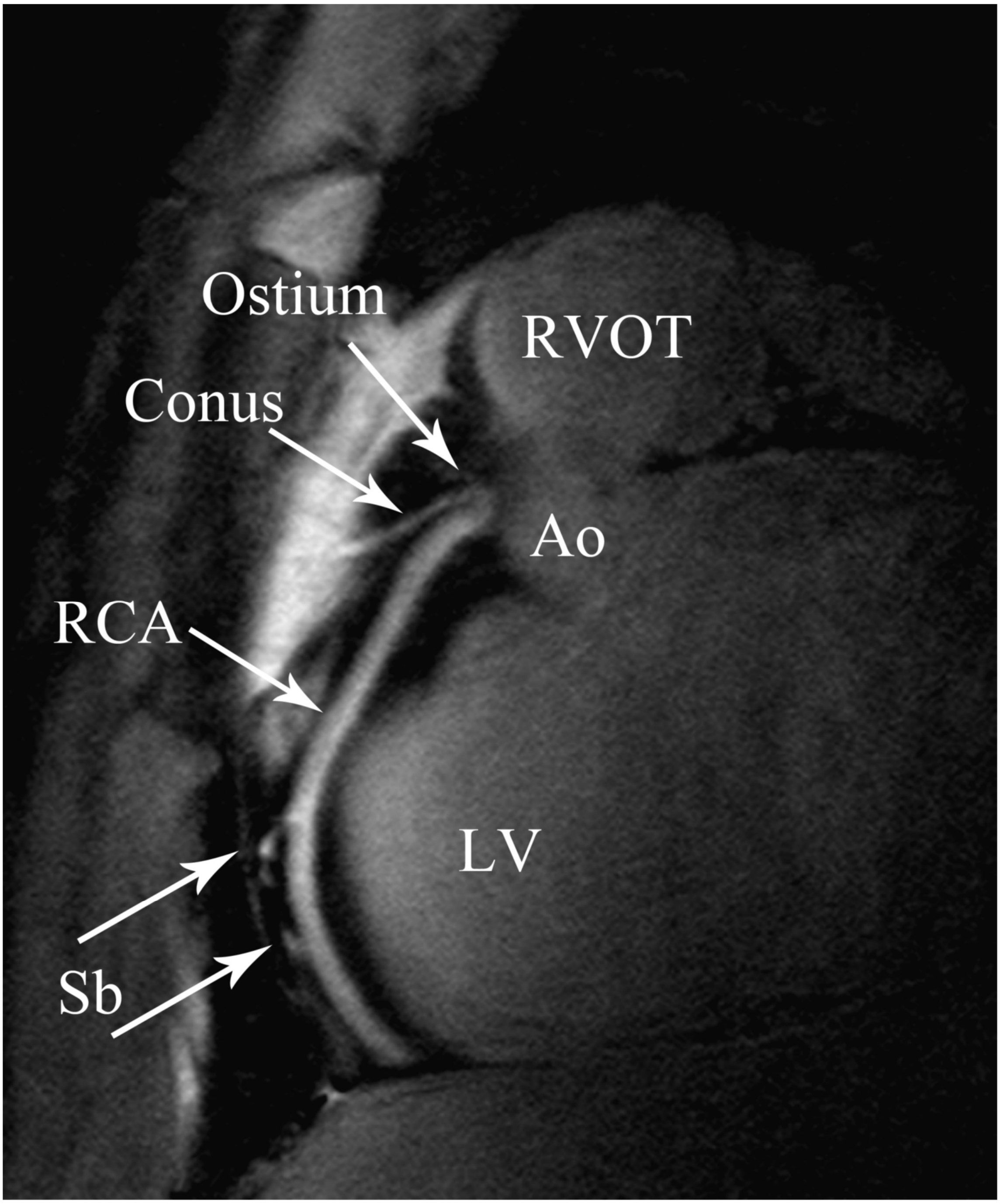

Figure 4. HR double oblique volume targeted plane parallel to the RCA. Note the well-defined borders of the RCA and fat suppression. In this figure, it is possible to identify the ostiummof the RCA, the conus, side branches (Sb), aortic root (Ao), left ventricle (LV), and right ventricular outflow tract (RVOT).

Discussion

The main finding of the present study is that HR bright blood coronary MRA at 7 T is feasible. High spatial resolution imaging demonstrated improved vessel delineation, as compared with bright blood imaging with lower spatial resolution.

Previously, coronary MRA at 7 T has been performed with bright blood imaging, showing increased SNR and CNR as compared with 3 T.[11] High VES is essential because well-defined borders of coronary arteries support improved identification of significant stenoses. The present study shows that VES is enhanced in higher spatial resolution imaging. As expected, SNR and CNR suffer from smaller voxel size, although CNR remained relatively high in HR images. Similar vessel length in HR and LR images supports the notion that CNR in HR coronary MRA is adequate for identification of the vessel. Thus, the gain in signal of higher field imaging can be used to successfully increase spatial resolution.

The actual loss in SNR in the HR sequence, as compared with the LR sequence, was lower than expected. Voxel size was reduced with a factor 5.5 in the HR sequence, whereas SNR decreased with an average factor of 3.4. This discrepancy cannot be fully explained by a difference in imaging sequences because the HR sequence merely has a somewhat longer echo time than the LR sequence does: 1.64 versus 1.3 milliseconds. This difference could even have resulted in a relatively lower SNR in HR images. Therefore, the explanation for this discrepancy likely resides in the image analysis. Because the epicardial fat and blood ROIs were divided by a single line (Fig. 1F), LR images had a larger partial volume effect at the border of the vessel wall. This has resulted in the inclusion of some blood in epicardial fat ROIs and vice versa. This also explains the relatively high standard deviation of SNR and CNR in the LR sequence, as compared with the HR sequence.

A limitation of the present study is that a 2-element coil was used for transmit/receive purposes. Recently, it has been shown that image quality can be significantly improved using transmit arrays.[8,14-16] Future studies involving, for example, optimization of transmit/receive coils could further boost the potentials of 7 T in coronary MRA. Furthermore, patient studies, including elderly and obese participants, are necessary to clarify the actual virtues of ultrahigh field imaging for detection of coronary artery stenosis. Another limitation of this study is the large navigator window that was used to reduce scanning time. Taking into account the high resolution, the reduction in the navigator window level could further increase VES by decreasing respiratory motion artefacts.

In conclusion, HR bright blood coronary MRA at 7 T is feasible and improves VES as compared with lower spatial resolution bright blood imaging.

References

1. Fihn SD, Gardin JM, Abrams J, et al. 2012 ACCF/AHA/ACP/AATS/PCNA/SCAI/STS guideline for the diagnosis and management of patients with stable ischemic heart disease: executive summary: a report of the American College of Cardiology Foundation/American Heart Association Task Force on Practice Guidelines, and the American College of Physicians, American Association for Thoracic Surgery, Preventive Cardiovascular Nurses Association, Society for Cardiovascular Angiography and Interventions, and Society of Thoracic Surgeons. Circulation. 2012;126:3097Y3137.
2. Kim WY, Danias PG, Stuber M, et al. Coronary magnetic resonance angiography for the detection of coronary stenoses. N Engl J Med. 2001;345:1863Y1869.
3. Kato S, Kitagawa K, Ishida N, et al. Assessment of coronary artery disease using magnetic resonance coronary angiography: a national multicenter trial. J Am Coll Cardiol. 2010;56:983Y991.
4. Cheng L, Ma L, Schoenhagen P, et al. Comparison of three-dimensional volume-targeted thin-slab FIESTA magnetic resonance angiography and 64-multidetector computed tomographic angiography for the identification of proximal coronary stenosis. Int J Cardiol. 2013;167:2969Y2976.
5. Sommer T, Hackenbroch M, Hofer U, et al. Coronary MR angiography at 3.0 T versus that at 1.5 T: initial results in patients suspected of having coronary artery disease. Radiology. 2005;234:718Y725.
6. Niendorf T, Graessl A, Thalhammer C, et al. Progress and promises of human cardiac magnetic resonance at ultrahigh fields: a physics perspective. J Magn Reson. 2013;229:208Y222.
7. Snyder CJ, DelaBarre L, Metzger GJ, et al. Initial results of cardiac imaging at 7 tesla. Magn Reson Med. 2009;61:517Y524.
8. Thalhammer C, Renz W, Winter L, et al. Two-dimensional sixteen channel transmit/receive coil array for cardiac MRI at 7.0 T: design, evaluation, and application. J Magn Reson Imaging. 2012;36:847Y857.
9. Vaughan JT, Snyder CJ, DelaBarre LJ, et al. Whole-body imaging at 7 T: preliminary results. Magn Reson Med. 2009;61:244Y248.
10. Versluis MJ, Tsekos N, Smith NB, et al. Simple RF design for human functional and morphological cardiac imaging at 7 tesla. J Magn Reson. 2009; 200:161Y166.
11. van Elderen SG, Versluis MJ, Westenberg JJ, et al. Right coronary MR angiography at 7 T: a direct quantitative and qualitative comparison with 3 T in young healthy volunteers. Radiology. 2010;257:254Y259.
12. van Elderen SG, Versluis MJ, Webb AG, et al. Initial results on in vivo human coronary MR angiography at 7 T. Magn Reson Med. 2009;62:1379Y1384.
13. Etienne A, Botnar RM, Van Muiswinkel AM, et al. ''Soap-Bubble'' visualization and quantitative analysis of 3D coronary magnetic resonance angiograms. Magn Reson Med. 2002;48:658Y666.
14. Winter L, Kellman P, Renz W, et al. Comparison of three multichannel transmit/receive radiofrequency coil configurations for anatomic and functional cardiac MRI at 7.0 T: implications for clinical imaging. Eur Radiol. 2012;22:2211Y2220.
15. Graessl A, Winter L, Thalhammer C, et al. Design, evaluation and application of an eight channel transmit/receive coil array for cardiac MRI at 7.0 T. Magn Reson Med. 2013;82:752Y759.
16. Graessl A, Renz W, Hezel F, et al. Modular 32-channel transceiver coil array for cardiac MRI at 7.0 T [Epub ahead of print]. Magn Reson Med. doi: 10.1002/mrm.24903.